JOURNAL OF Applied Polymer SCIENCE

Special Issue: Manufacturing of Advanced Biodegradable Polymeric Components

Guest Editors: Prof. Roberto Pantani (University of Salerno) and
Prof. Lih-Sheng Turng (University of Wisconsin–Madison)

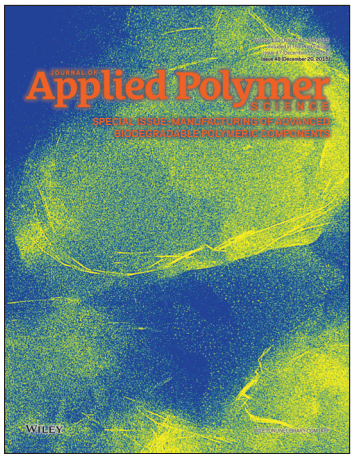

EDITORIAL

REVIEWS

ARTICLES

JOURNAL OF Applied Polymer SCIENCE

Special Issue: Manufacturing of Advanced Biodegradable Polymeric Components

Guest Editors: Prof. Roberto Pantani (University of Salerno) and Prof. Lih-Sheng Turng (University of Wisconsin–Madison)

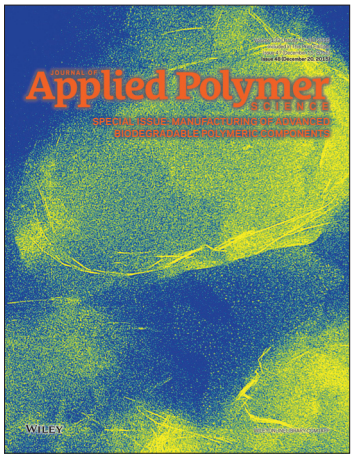

Rotational molding of biodegradable composites obtained with PLA reinforced by the wooden backbone of opuntia ficus indica cladodes
A. Greco and A. Maffezzoli, *J. Appl. Polym. Sci.* 2015, **DOI:** 10.1002/app.42447

Foam injection molding of poly(lactic) acid: Effect of back pressure on morphology and mechanical properties
V. Volpe and R. Pantani, *J. Appl. Polym. Sci.* 2015, **DOI:** 10.1002/app.42612

Modification and extrusion coating of polylactic acid films
H.-Y. Cheng, Y.-J. Yang, S.-C. Li, J.-Y. Hong and G.-W. Jang, *J. Appl. Polym. Sci.* 2015, **DOI:** 10.1002/app.42472

Processing and properties of biodegradable compounds based on aliphatic polyesters
M. R. Nobile, P. Cerruti, M. Malinconico and R. Pantani, *J. Appl. Polym. Sci.* 2015, **DOI:** 10.1002/app.42481

Journal of Applied Polymer Science

Foaming behavior of bio-based blends based on thermoplastic gelatin and poly(butylene succinate)

Maria Oliviero, Luigi Sorrentino, Livia Cafiero, Barbara Galzerano, Andrea Sorrentino, Salvatore Iannace

Institute for Polymers, Composite and Biomaterials (IPCB-CNR), Piazzale Enrico Fermi 1, 80055 Portici (Napoli), Italy

Correspondence to: A. Sorrentino (E-mail: andrea.sorrentino@cnr.it)

ABSTRACT: Biodegradable thermoplastic gelatin/poly(butylene succinate) (TPG/PBS) foams were prepared by melt mixing and subsequent batch foaming with supercritical CO_2. Shear viscosity and calorimetric properties of the various blends were investigated using a rotational rheometer and a differential scanning calorimeter, respectively. TPG/PBS blends show poor miscibility at all blend ratios. The addition of PBS reduced the melt viscosity and increased both the CO_2 diffusivity and the thermal stability of TPG. Results from foaming experiments show that the blend foams exhibit smaller cell size and higher cell density compared to the neat TPG foam due to the lower melt viscosity and to their lower gas barrier. © 2015 Wiley Periodicals, Inc. J. Appl. Polym. Sci. **2015**, *132*, 42704.

KEYWORDS: biopolymers and renewable polymers; blends; foams; morphology; properties and characterization

Received 24 March 2015; accepted 7 July 2015

DOI: 10.1002/app.42704

INTRODUCTION

The development of biobased polymer foams is of worldwide interest due to their environmentally friendly nature and their potential use in different technical applications.[1–3] "Biobased polymer" refers to polymeric materials obtained from renewable resources that can be processed to obtain plastic-like products with desired structural and functional properties. A wide variety of biobased polymers are available in nature, including proteins (wool, silk, casein, and zein), oils and fats, lignin, as well as polymers derived from monomeric components obtained from renewable resources.[4,5] In this contest, gelatin, a protein derived from the partial hydrolysis of collagen, has shown a good potential as substitute of petroleum based plastics. Porcine and bovine skins are the main sources of gelatin and widely utilized in food manufacturing.[6] Alternative sources, such as fish, chicken and duck based poultry have also considered in the last decades.[7,8] Actually, more than half the animal byproducts are not suitable for normal consumption. Additionally, traditional markets for food derived from byproducts have gradually been disappearing because of health concerns. It means that a valuable source of potential revenue is lost, and the cost of disposing of these products is rapidly increasing.[9] In response to these problems, food processors have directed their marketing and research efforts towards maximizing its use in nonfood applications.[10]

It has been shown that gelatin can be processed by conventional dry mixing techniques, after being adequately plasticized, to obtain the so called thermoplasticized gelatin (TPG).[11] TPG is characterized by interesting mechanical properties and excellent barrier properties to oxygen. As a major drawback, it has a strong sensitivity to moisture, which can heavily decrease its barrier as well as its thermomechanical properties.[11] Blending with other biodegradable polymers may be a viable solution to this issue. Examples reported in literature show that the mechanical and water barrier properties of gelatin based films have been improved by "in solution mixing" with high molecular weight carbohydrates such as starch and chitosan,[12–14] other proteins such as soy protein,[15] synthetic polymers such as poly (vinyl alcohol)[16] oligosaccharides and some organic acids.[17,18] The possibility of obtaining stable foams with a good cellular morphology is another important drawback for the use of plasticized gelatin in conventional applications. The low permeability to gas, the low crystallinity and the usually high viscosity are important faults to be mitigated.

PBS is a semicrystalline polymer with excellent biodegradability, good processability, and mechanical properties similar to those of polyethylene. The relatively high cost and some performance shortcomings, such as low melt strength and high permeability to gases have strongly limited its applications. Also in this case, blending with other biodegradable polymers, such as PLA,[19] natural fibers,[20] starch,[21] novatein protein,[22] and soy protein[15] have been proposed to enhance its properties. PBS was also investigated with the aim to produce biodegradable foams. These foams have recently awakened interests of scientists and

researchers because of its biocompatibility, low density, strong energy absorption capability, as well as good sound and thermal insulation.[23]

Zhang *et al.*[24] studied the effect of the processing conditions on the morphology of PBS foams. Authors used ammonium bicarbonate as foaming agent and found that a low density foam can only be obtained by adding talc as nucleating agent. Since conventional PBS grades do not show good foaming properties, efforts have been made to improve the elongational viscosity of the polymer to improve its foamability. Son *et al.*[25] obtained PBS foams using supercritical CO_2 as blowing agent. Authors used a reactive compounding technique to increase the molecular weight of PBS and its melt strength. Similarly, Lim *et al.*[26] used two types of polyisocyanate as branching agents into PBS matrix. Bahari *et al.*[27] investigated the effects of radiation on the crosslinking of PBS foams and on its biodegradation. Guan *et al.*[28] used dicumyl peroxide and trimethylolpropane trimethacrylate to prepare high viscosity PBS and were able to prepared PBS foams by compression moulding.

An interesting strategy, less investigated, to improve the foamability of biodegradable polymers such as PBS and TPG can be represented by their blending to adjust the rheological properties, to enhance cell nucleation, and to tailor the diffusivity and solubility of the blowing agent. To that purpose, in this paper the development of foams based on TPG/PBS biobased blends is reported. TPG/PBS blends with different compositions have been prepared and characterized using thermal and rheological analyses. Blends have been foamed by using CO_2 as a blowing agent. A correlation between foam morphology and processing conditions has been proposed in light of the thermal and rheological properties of the starting blends.

MATERIALS AND METHODS

Materials

Gelatin from bovine skin type B (CAS 9000-70-8) and glycerol (CAS 56-81-5), used as plasticizer for the preparation of TPG, were purchased from Sigma-Aldrich. PBS Bionolle 1903 produced by Showa High Polymers was supplied by Toyo Plastics. CO_2, used as physical blowing agent for gas foaming experiments was purchased from Air Liquide.

Samples Preparation

Various formulations of TPG/PBS were prepared using a two-step procedure. The initial step aimed at the destructurization and plasticization of the gelatin protein was carried out using an internal mixer (Rheomix 600 Haake) controlled by a measuring drive unit (Haake Rheocord). In particular, 50 g of gelatin powder were mixed with 20 wt % of glycerol at 80°C, 60 rpm for 6 min. TPG was then extracted from the mixer and granulated for further processing. Subsequently, TPG/PBS blends were obtained with the same mixing equipment at 120°C, 80 rpm for 6 min. Different TPG/PBS compositions, ranging from 80/20 to 20/80 wt/wt %, were prepared. A compression molding press was used to prepare specimens for both shear rheological measurements and foaming experiments. Polymer slabs were molded at 120°C under a pressure of 30 bar in a hot plate press (P300 Collin). Processing times were limited to 8–10 min in order to prevent any thermal degradation of polymers.

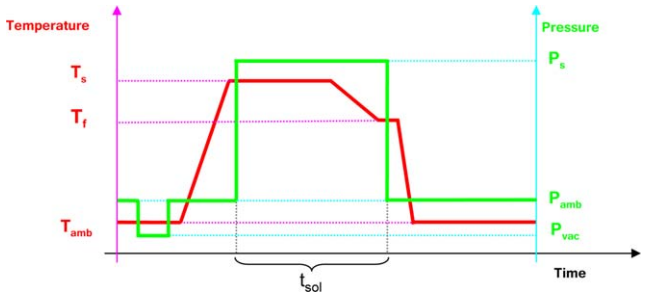

Figure 1. Schematic representation of the temperature/pressure history imposed to the samples in the foaming tests. T_s is the solubilization temperature, T_f is the foaming temperature, T_{amb} is the room temperature, t_{sol} is the solubilization time, P_s is the solubilization pressure, P_{amb} is the room pressure, P_{vac} is the vacuum pressure. [Color figure can be viewed in the online issue, which is available at wileyonlinelibrary.com.]

Samples Characterization

Thermal Analysis. The thermal characteristics of TPG, PBS, and their blends were determined under a nitrogen atmosphere using a differential scanning calorimeter (DSC Q1000) (TA instrument). Few micrograms (approximately 5–7 mg) were cut from the molded slabs and tested through a heating–cooling–heating procedure, with a scan rate of 10°C/min. Temperature scan was performed from −50 to 180°C for all samples. Glass transition temperature (T_g), melting temperature (T_m), and crystallization temperature (T_c) were all determined from the detected thermograms. In particular, T_g was determined as the onset of the DSC signal from the baseline shift, T_m as the onset of the endothermic melting peak, and T_c as the onset of the exothermic peak.

Rheological Measurements. Rheological experiments were performed using a stress controlled rotational rheometer (HAAKE RheoScope MARS III) equipped with 20 mm parallel plates and using a gap thickness of 0.15 mm. The tests were performed at 120°C under dry nitrogen atmosphere, and with a frequency sweep from 0.05 to 100 Hz. A fixed strain of $\gamma = 0.1\%$ was chosen for all samples in order to operate in the linear viscoelastic region.

Foaming

Batch Foaming Experiments. Foaming experiments were carried out by using a batch process by expanding disc-shaped samples with 10 mm in diameter and 1 mm in thickness. In each experiment, the samples were placed inside a high-pressure vessel that was firstly evacuated for about 10 min. After that step, the vessel was heated at the desired temperature (T_s) and immediately filled with CO_2 up to reach a constant pressure (P_s) for various time intervals (t_s). The vessel was then cooled to the desired foaming temperature (T_f) and the pressure quickly released to allow sample foaming. Finally, in order to stabilize the cellular structure, the samples were immediately removed from the vessel and allowed to cool at room conditions. A sketch of the temperature/pressure history imposed to the samples is reported in Figure 1.

Table I. Experimental Conditions used for the Preparation of Foams

Test number	T_s (°C)	P_s (bar)	T_f (°C)
1	100	65	100
2	120	65	100
3	120	85	80
4	120	85	75
5	120	85	100
6	100	85	100

Among all the experiments carried out, the test conditions listed in Table I were selected to elucidate the effect of temperature, pressure and time on the development of the cellular morphology during the foaming stage.

Foam Characterization. The analysis of the foamed specimens included an investigation of the foam morphology with a special emphasis on the relation between the mean cell size and the blend composition.

Foam morphologies were characterized by scanning electron microscopy (SEM) with a Quanta 200 FEG. Samples were fractured in liquid nitrogen and cross sections were gold-sputtered before being observed by SEM (operating at an accelerating voltage of 20 kV and at various magnifications). The mean cell size was evaluated by Image J software (from NIH). A minimum of 100 pores for each sample were selected from the micrographs and analyzed by assuming a spherical shape of pores.

The porosity Φ of each sample was determined using eq. (1):

$$\Phi = \left[1 - \frac{\rho_f}{\rho_b}\right] \times 100 \quad (1)$$

where ρ_f is the foam density and ρ_b the bulk density. The density of foams was measured with a hydrostatic balance according to ASTM D792. Because TPG is soluble in water, tetrahydrofuran was used as liquid media in measurements. The reported foam porosity was obtained by averaging between the results from three specimens for each composition and foaming conditions. Highly consistent results with a standard deviation of less than 4% were obtained.

RESULTS AND DISCUSSION

Thermal Behavior of the TPG/PBS Blends

Figure 2(A,B) show the first heating and the subsequent cooling thermograms for all the analyzed samples, respectively. The DSC heating curve of TPG shows an endothermic peak in the range 120–180°C, which corresponds to helix-coil transitions in gelatin, as reported by Vanin *et al.*[29] for dehydrated gelatin–glycerol systems. The cooling curve from the melt state does not show any reorganization or crystallization peak, which indicates that the sample retain its fully amorphous state. PBS shows multimelting endotherms in the range 100–120°C. In general, the melting behavior of PBS depends on several factors, such as the thermomechanical history, molecular weight, and sample conditioning.[30] Yasuniwa *et al.*[31] found that PBS, nonisothermally crystallized from the melt, shows three endothermic peaks, which were attributed to the melting, recrystallization, and remelting processes undergone during heating. Yoo *et al.*[32] showed that the middle peak correspond to the melting of the original lamellae formed during the previous crystallization step, whereas the highest melting peak correspond to the melting of the structures formed during the heating step. The location of melting peaks for the two blends is almost the same of the pure PBS.

Table II provides a summary of the DSC results, reporting the glass transition temperature, the melting temperature, and the degree of crystallinity of the different samples. The crystallization temperature of the PBS component in the blends shows an evident increase, which indicates that gelatin have a nucleating effect on PBS thus favoring solidification during the melt process. However, the PBS in the blends showed a change in

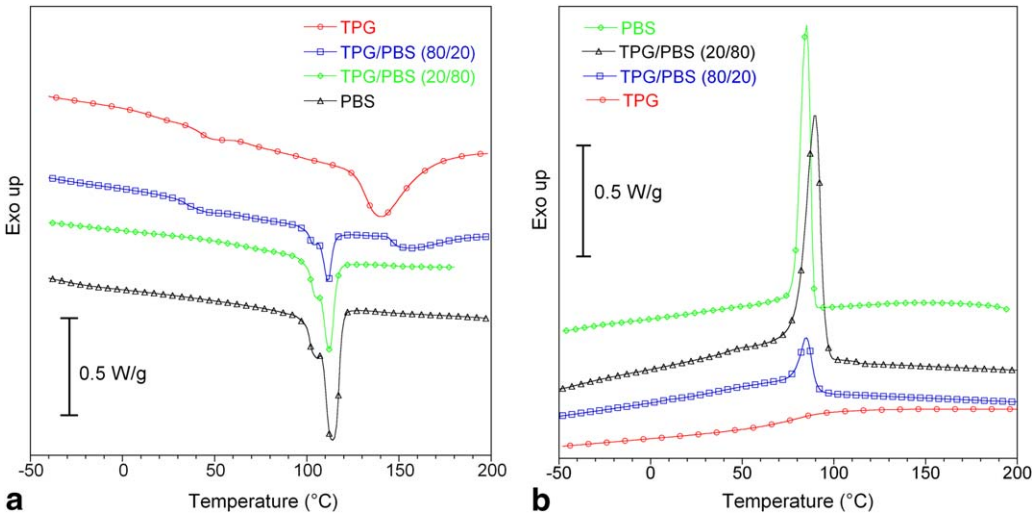

Figure 2. (A) Heating endotherms for TPG/PBS blends and (B) cooling extherms for TPG/PBS blends. [Color figure can be viewed in the online issue, which is available at wileyonlinelibrary.com.]

Table II. Calorimetric Data for the Neat TPG, PBS, and Their Blends

TPG/PBS (wt %/wt %)	TPG	PBS				
	T_g (°C)	T_g (°C)	T_m (°C)	T_c (°C)	ΔH_f (J/g)	X_c (%) (PBS)
100/0	43	-		-	-	-
80/20	34	-	111	88	12	56
20/80	27	-	111	86	52	58
0/100	-	−32	113	84	68	61

enthalpy upon crystallization (ΔH_c) almost proportional to the PBS content (Table II). The degree of crystallinity of PBS ($X_{c,\mathrm{PBS}}$) in each blend was calculated using eq. 2:

$$X_{c,\mathrm{PBS}} = \left(\frac{\Delta H_f}{W_{\mathrm{PBS}}}\right)\frac{1}{\Delta H^0_{f,\mathrm{PBS}}} \tag{2}$$

where ΔH_f is the heat of fusion (in J/g units) calculated by integrating the area under the melting peak of each thermogram (see Table II), W_{PBS} is the mass fraction of PBS in the TPG/PBS blend, and ΔH^0_f is the heat of fusion for the PBS 100% crystalline taken as 110.3 J/g.[33]

The calculated results, plotted in Figure 3(A), show that the PBS crystallinity remains fairly constant regardless of the amount of TPG in the blends. Similar observation has also been reported on poly (butylene succinate)/polylactide blends by Wu *et al.*[34] This provides cab be taken as an evidence for the very limited miscibility of TPG and PBS.

In all of the enthalpic curves, only the T_g of TPG results clearly identifiable. Probably, for the PBS, the small change in the specific heat capacity and the characteristic low T_g temperature (below −30°C) makes difficult its detection. The T_g of TPG in the blend as function of PBS content is depicted graphically in Figure 3(B). As can be seen, the T_g was observed to be depressed from 43°C of the pure TPG to 34 and 27°C with the addition of 20 and 80% of PBS, respectively. The composition dependence of the glass transition temperature in a polymeric blend is often modeled using the Gordon Taylor (G–T)[35] relationship [eq. (3)]:

$$T_g = \frac{W_1 \cdot T_{g1} + k \cdot W_2 \cdot T_{g2}}{W_1 + k \cdot W_2} \tag{3}$$

where W_1 and W_2 are the weight fractions of two blend components, and T_{g1} and T_{g2} are the respective glass transition temperatures of the neat components. The parameter k is represented by $\Delta\alpha_2/\Delta\alpha_1$, where $\Delta\alpha_i$ is the change between the liquid and glassy thermal expansion coefficient at T_{gi}.

Usually, k is used as fitting parameter: a value close to unity indicates good miscibility between blend components, whereas a too high or low value for k indicates limited miscibility.[35] The comparison between the T_g of the TPG with the G–T model is depicted graphically in Figure 3(B). It must be noted that for neat PBS, the literature T_g value (−32°C) was used. As showed in Figure 3(B), a good agreement between the observed T_g and the G–T model is obtained for $K = 0.1$, indicating a very limited miscibility of TPG and PBS components.

Rheological Characterization

To develop a good foam morphology, a polymeric material with a suitable melt strength is needed. The melt strength represents the resistance of the polymer melt to stretching and is related to the molecular chain entanglements and its resistance to untangling under strain. Polymers with low melt strength values are not able to bear the stretching forces occurring on cell walls

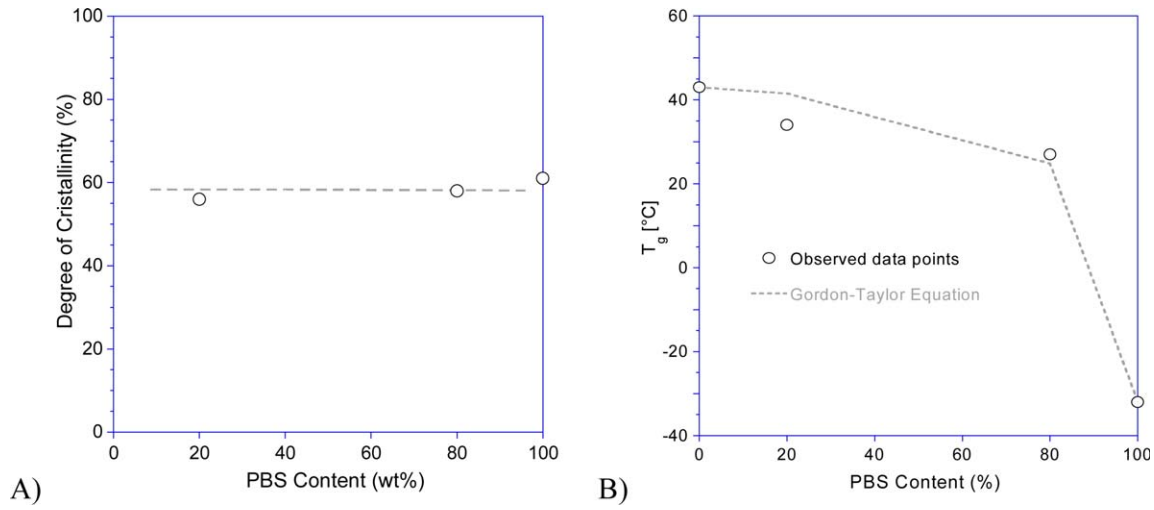

Figure 3. (A) Degree of crystallinity of the PBS fraction for the various blends and (B) T_g of the TPG fraction as function of the PBS content. [Color figure can be viewed in the online issue, which is available at wileyonlinelibrary.com.]

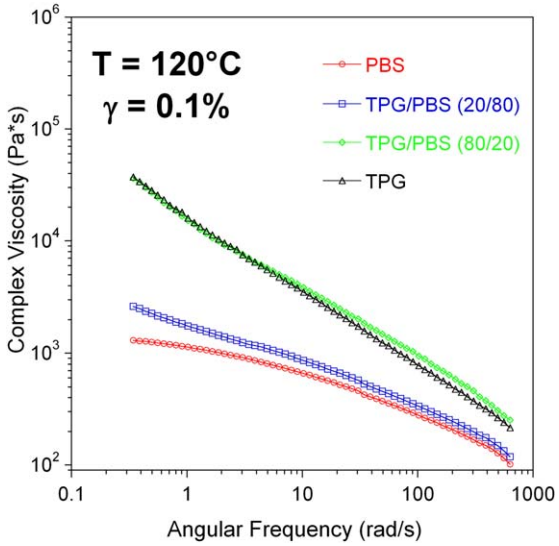

Figure 4. Complex viscosity at strain of $\gamma = 0.1\%$ as a function of the angular frequency at 120°C. [Color figure can be viewed in the online issue, which is available at wileyonlinelibrary.com.]

during the bubble expansion. On the contrary, high melt strength can hinder the bubble growth. The experimental determination of the transient extensional viscosity of foam is fraught with all of the problems characteristic of a two phase system. Despite the large difference between them, it is quite common to use the shear properties of polymer melts as a reference for its extensional rheological characteristics at high temperatures.[36,37] They are more simple to be carried out and provide a complete picture of the polymer blend properties in terms of morphology and compatibilization of the components.

In our case, rheological measurements were performed to evaluate the complex viscosity of the TPG/PBS blends at the foaming temperature (120°C). In particular, Figure 4 shows the changes in the complex viscosity of samples as a function of the oscillation frequency, at a fixed strain of $\gamma = 0.1\%$. For all samples, the complex viscosity decreased with both increasing frequency and increasing PBS content. TPG and TPG/PBS blends showed a shear thinning behavior in the entire frequency range with log (η^*) versus log (f) curve decreasing with a constant slope. Conversely, PBS showed a transition from an end Newtonian plateau. These phenomena suggest that TPG molecules in the blends are able to form of an interconnected network structure.

In Figure 5(A,B), the changes in the storage modulus (G') and the loss modulus (G'') of samples are shown versus the oscillation frequency, at a fixed strain of $\gamma = 0.1\%$. As expected, all samples showed an increase of G' and G'' with the frequency. The values of G' increased with the TPG content, which implied that the melt elasticity of the blends is enhanced by the presence of TPG molecules. The G'' curves of various samples had similar trend with the G' curves. However, in particular for the sample TPG/PBS (20/80), the increase of G'' was lower than that of G', indicating that the addition of TPG mainly increased the elastic component of the viscoelasticity with respect to the viscous one. This is another evidence of the improvement in the relaxation properties (in particular the melt elasticity) induced by the TPG addition to PBS.

A rough estimation of the melt strength can be obtained by looking at the shift of the crossover point of the G'' and G' curves. The crossover point, in fact, gives an indication of the average molecular weight and breadth of the molecular weight distribution of the sample. Long-chain branching or entanglement, which is probably present in the TPG, increases the elasticity of the melt and shifts the crossover point to lower frequencies. The inverse of the crossover frequency (f_{cr}), which is equivalent to a characteristic relaxation time of the material, is reported in Table III.

It is clear from the Table III that samples elasticity increases with the TPG content. Longer relaxation times indicate higher melt elasticity and, indirectly, high molecular entanglement. It is also true that the enhancement of the elasticity can also be due to the presence of a broader molecular weight distribution. However, in our case, the increases in both elastic modulus and viscosity are a clear confirmation of an extensive molecular entanglement.

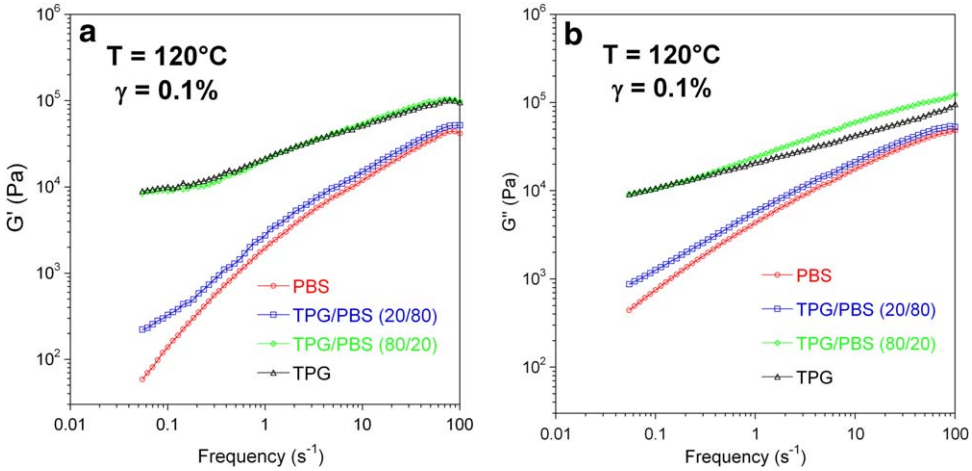

Figure 5. (A) Storage modulus (G'); (B) loss modulus (G'') at strain of $\gamma = 0.1\%$ as a function of the frequency at 120°C. [Color figure can be viewed in the online issue, which is available at wileyonlinelibrary.com.]

Table III. Elasticity Parameters of the Neat TPG, PBS, and Their Blends

TPG/PBS (wt %/wt %)	$1/f_{cr}$ (s)
100/0	1.70
80/20	0.50
20/80	0.02
0/100	0.01

Batch Foaming

Porosity. Batch-foaming provides a straightforward method to evaluate the foamability of polymers. As a first indicator of the foamability of a polymer, the foam porosity was evaluated on neat polymers and blends for all the test conditions used. In Figure 6(A–C), the effect of the sorption temperature (T_s), sorption pressure (P_s), and foaming temperature (T_f), respectively, on the foam porosity are reported.

As shown in Figure 6, the foam porosity appears to depend on both the blend composition and the foaming parameters. In particular, in Figure 6(A) is evident that a solubilization temperature higher than the melt temperature of the PBS favored the expandability of the blends and led to an increase in foam porosity. In contrast, only the TPG foams exhibited a lower porosity at higher T_s. Figure 6(B) shows that an increase of the solubilization pressure resulted in an increased porosity for all samples. This is probably due to the higher solubilization of CO_2 induced by the higher pressure at constant temperature. Finally, the decrease of the foaming temperature, keeping constant the solubilization pressure and temperature, show a strong porosity reduction for all the blends investigated [Figure 6(C)].

Foam Morphology and Cell Size. Samples of TPG/PBS blends have been foamed below and above the melting temperature of PBS to show how the blend composition and the foaming temperature can affect the final cellular morphology. The SEM analysis confirmed that PBS and TPG polymers are practically immiscible, since spherical domains as dispersed phase were detected in all blends. The size of PBS domains in TPG/PBS (80/20) composition was between 2.5 and 9 μm while the size of TPG domains in TPG/PBS (20/80) sample was between 3.0 and 13 μm. After foaming, the dispersed phase was still evident in all foamed blends.

The foam morphology was strongly influenced by both blend morphology and sorption conditions. TPG has shown a well-defined cellular structures, with cells between 15 and 40 μm in size [Figure 7(A)]. Since at 120°C PBS was completely melted, the absence of crystalline phase and the low viscosity (see Figure 4) allowed the nucleation and growth of cells and the development of a microcellular morphology. As a result, PBS developed a very good foam morphology, with a mean cell size of 13 μm [Figure 7(D)]. The foamability of PBS was exploited to improve the cellular morphology of the TPG based blend. In particular, it is remarkable that albeit the viscosity of the TPG/PBS (80/20)

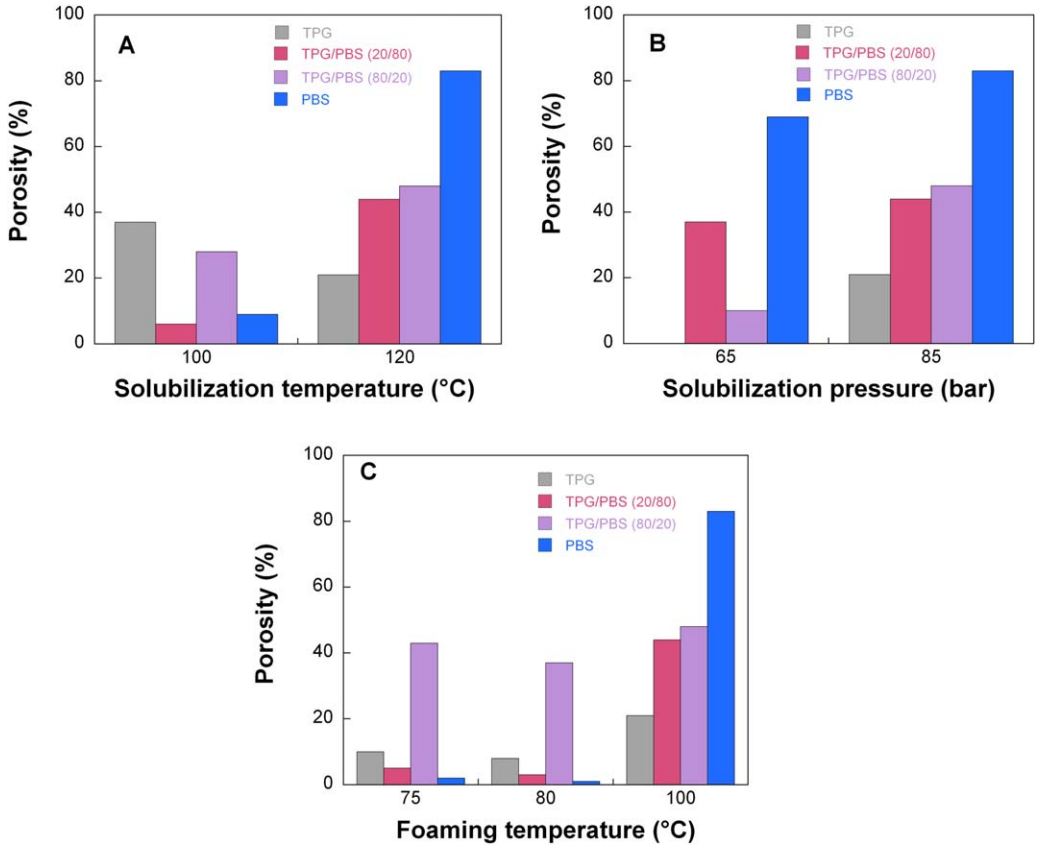

Figure 6. Porosity (%) of the TPG/PBS blends as a function of (A) solubilization temperature (tests 5 and 6); (B) solubilization pressure (tests 2 and 5), and (C) foaming temperature (tests 3, 4, and 5). [Color figure can be viewed in the online issue, which is available at wileyonlinelibrary.com.]

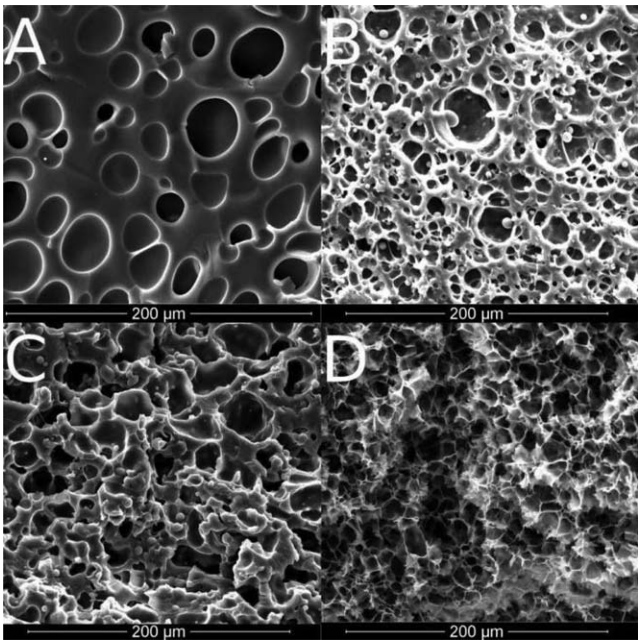

Figure 7. SEM micrographs of foams obtained in test 5: (A) TPG; (B) (TPG/PBS) (80/20); (C) (TPG/PBS) (20/80); and (D) PBS.

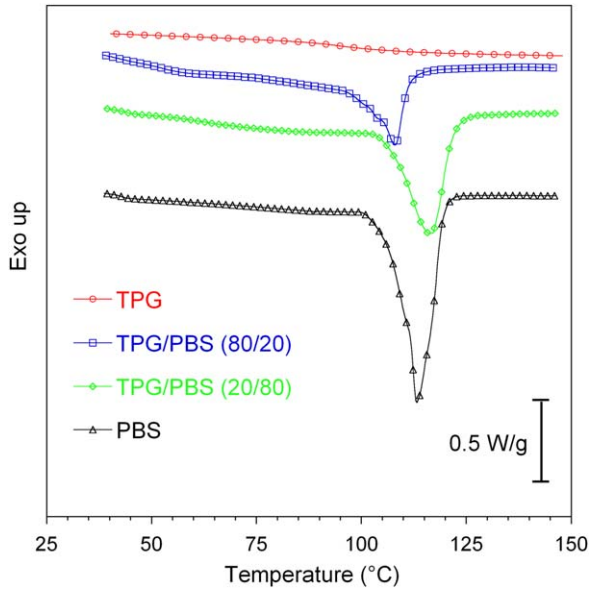

Figure 9. DSC test of the samples after test 5 foaming experiment. [Color figure can be viewed in the online issue, which is available at wileyonlinelibrary.com.]

blend was equal to that of TPG (see Figure 4), the presence of PBS strongly improved the cellular morphology of the blend with respect to TPG and allowed the development of a good cellular morphology through the nucleation and growth of small cells. The TPG/PBS (20/80) blend also showed a good cellular structure but the mean cell size was slightly higher (17 μm) than that of PBS foam.

The morphology of TPG/PBS (80/20) sample foamed at 100°C, thus below the melting temperature of PBS, is pictured in Figure 8. As evident the presence of PBS did not significantly improve the cellular morphology with respect to TPG [Figure 6(A)]. This was attributed to the combined effect of the higher elasticity of the matrix, the lower CO_2 uptake and to the presence of a crystalline phase in the dispersed phase at 100°C with respect to 120°C. In fact, as reported by Sato *et al.*[38] who investigated the transport properties of carbon dioxide in PBS, below the melting temperature of PBS the gas uptake was strongly reduced by the presence of crystals. In particular, at 90°C (a condition very similar to that used in the present work) the gas uptake at 6.7 MPa was equal to 4.7% and to 7.1% in the crystallized and in the totally amorphous polymers, respectively (uptake values extrapolated from data in Sato *et al.*[31] by means of linear regression). The large difference in the gas uptake can have a significant effect in hindering the development of a cellular structure during foaming [Figure 7(D)]. A higher CO_2 content, in fact, can increase the plasticization of the polymer, reduce its viscosity and increase the thermodynamic instability for bubble nucleation. Therefore, the contribution of PBS to the foaming of TPG can be maximized by minimizing the presence of crystals in the dispersed phase.

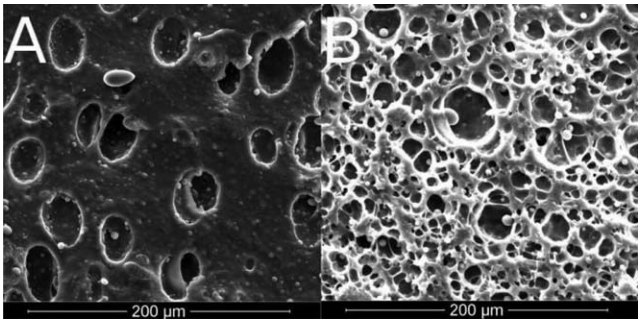

Figure 8. SEM micrographs of TPG/PBS (80/20) foams: (A) test 6 and (B) test 5.

Figure 9 shows the melting behavior of samples foamed in the test 5 conditions. As evident, all samples show a higher degree of crystallinity with respect to the un-foamed materials. The range for the degree of crystallinity of PBS is 55–60% depending on crystallization conditions, whereas samples processed under CO_2 showed values in the region of 70%. The increase in crystallinity is due to the relative increment of the segmental mobility of PBS macromolecules allowed by the CO_2 plasticisation.[39] The increased crystallinity can help to stabilize the cellular morphology but also hinder the development of a high porosity.

Discussion

Polymer materials are used in a wide variety of low cost, throw-away, applications such as disposable packaging of fast-food and insulation material. The increased requests for renewable and agro-based materials in industrial applications is forcing manufactures to develop new approaches and processes able to overcome their intrinsic problems such as high cost, limited availability, inferior performance and variable source/compositions.[40] In particular, the high cost and the poor processability have suggested the possibility to use these materials for making

biodegradable foams. Foam processing such as extrusion and injection molding, in fact, offer unique advantages such as low material usage, low shear deformation and reduced temperature and pressure. As showed before, the addition of a commercial PBS to the thermoplastic gelatin have a positive effect on its foamability. Unlike more conventional leaching process, foaming with physical blowing agent, offers several potential advantages: namely, improved control over material structure and porosity, and versatility in the resulting material properties. Potentially, it is possible to obtain foams with specific properties such as appropriate pore size, sufficient porosity and high interconnectivity, adequate mechanical stability, and tuned biodegradation rate. Salerno *et al.*[11] have showed that thermoplastic gelatin can be foamed in the temperature range between 50 and 140°C obtaining closed pores morphology. In our case, the size and the number of the pores could be controlled by changing the process conditions or by changing the PBS concentration. Foams with highly regular and interconnected pore structure, possessing relative densities in the range of 0.8–0.5, densities as low as 500 mg/cc were produced by using this approach. Undoubtedly, their properties originating from their controlled structure pave the way to a much broader range of applications, and open a new dimension for renewable materials. However, a further optimization of the micro-architecture of the porous structure requires supplementary investigation of processing/structure/property relationships with respect to the specific system selected.

CONCLUSIONS

PBS was blended with TPG with the aim to improve the foaming properties of these materials without affecting their biodegradability. Phase morphology and properties for binary blends of TPG and PBS were hence studied. It was found from SEM and thermal analysis, that TPG and PBS form a practically immiscible blend. The thermal characterization also showed that the crystallinity of PBS in the blends is almost comparable with that of pure PBS, thus it is unaffected by the presence of TPG. The rheological test results revealed that TPG/PBS blends show a higher viscosity than pure PBS due to the prevalence of the viscoelastic properties of TPG. This affected the foaming behavior of the blends. The foaming behavior of neat polymers and the their blends was investigated by means of the batch foaming process and supercritical carbon dioxide was used as physical blowing agent. The very poor miscibility of the polymers was preserved in foams and it helped in governing the cellular structure. Foamed blends showed smaller cell size and higher cell density compared to neat TPG foams. This means that small amounts of PBS can be employed to improve the foamability of TPG. In any case, the foam morphology resulted function of both blend composition and foam conditions. It means that the desired porosity of the foams can be obtained by a correct choosing of the processing conditions.

REFERENCES

1. Krochta, J. M.; De Mulder Johnston, C. *Food Technol.* **1997**, *51*, 61.
2. Pantani, R.; Sorrentino, A. *Polym. Degrad. Stab.* **2013**, *98*, 1089.
3. Giuliana, G.; Sorrentino, A. *Green Chem.* **2015**, *17*, 2610.
4. Imre, B.; Pukánszky, B. *Eur. Polym. J.* **2013**, *49*, 1215.
5. Verdolotti, L.; Lavorgna, M.; Oliviero, M.; Sorrentino, A.; Iozzino, V.; Buonocore, G.; Iannace, S. *ACS Sustain. Chem. Eng.* **2014**, *2*, 254.
6. Kittiphattanabawon, P.; Benjakul, S.; Visessanguan, W.; Shahidi, F. *Food Hydrocoll.* **2010**, *24*, 164.
7. Gomez-Guillen, M. C.; Gimenez, B.; Lopez-Caballero, M. E.; Montero, M. P. *Food Hydrocoll.* **2011**, *25*, 1813.
8. Karim, A. A.; Bhat, R. *Food Hydrocoll.* **2009**, *23*, 563.
9. Rivera, J. A.; Sebranek, J. G.; Rust, R. E.; Tabatabai, L. B. *Meat Sci.* **2000**, *55*, 53.
10. Chiellini, E.; Cinelli, P.; Fernandes, E. G.; Kenawy, El-R. S.; Lazzeri, A. *Biomacromolecules* **2001**, *2*, 806.
11. Salerno, A.; Oliviero, M.; Di Maio, E.; Iannace, S. *Int. Polym. Proc.* **2007**, *22*, 480.
12. Arvanitoyannis, I.; Psomiadou, E.; Nakayama, A.; Aiba, S.; Yamamoto, N. *Food Chem.* **1997**, *60*, 593.
13. Arvanitoyannis, I.; Nakayama, A.; Aiba, S. *Carbohydr. Polym.* **1998**, *36*, 371.
14. Cao, N.; Yang, X.; Fu, Y. *Food Hydrocoll.* **2009**, *23*, 729.
15. Li, Yi-D.; Zeng, J. B.; Wang, X. L.; Yang, K. K.; Wang, Y. Z. *Biomacromolecules* **2008**, *9*, 3157.
16. Mendieta-Taboada, O.; Sobral, P. J.; Carvalho, R. A.; Monica, A.; Habitante, B. Q. *Food Hydrocoll.* **2008**, *22*, 1485.
17. Karnnet, S.; Potiyaraj, P.; Pimpan, V. *Polym. Degrad. Stab.* **2005**, *90*, 106.
18. Peña, C.; de la Caba, K.; Eceiza, A.; Ruseckaite, R.; Mondragon, I. *Bioresour. Technol.* **2010**, *101*, 6836.
19. Yokohara, T.; Yamaguchi, M. *Eur. Polym. J.* **2008**, *44*, 677.
20. Liu, L.; Yu, J.; Cheng, L.; Yang, X. *Polym. Degrad. Stab.* **2009**, *94*, 90.
21. Zeng, J. B.; Jiao, L.; Li, Y. D.; Srinivasan, M.; Li, T.; Wang, Y. Z. *Carbohydr. Polym.* **2011**, *83* 762.
22. Marsilla, K. I. K.; Verbeek, C. J. R. *Int. J. Chem. Eng. Appl.* **2013**, *4*, 106.
23. Jeon, B.; Kim, H. K.; Cha, S. W.; Lee, S. J.; Han, M-S.; Lee, K. S. *Int. J. Precision Eng. Manufact.* **2013**, *14*, 679.
24. Zhang, Y.; Lu, B.; Lv, F.; Guo, W.; Ji, J.; Chu, P. K.; Zhang, C. *J. Appl. Polym. Sci.* **2012**, *126*, 756.
25. Son, J. M.; Song, K. B.; Kang, B. W.; Lee, K. H. *Polymer (Korea)* **2011**, *36*, 34.
26. Lim, S. K.; Jang, S. G.; Lee, S. I.; Lee, K. H.; In-Joo Chin, I. J. *Macromol. Res.* **2008**, *16*, 218.
27. Bahari, K.; Mitomo, H.; Enjoji, T.; Yoshii, F.; Makuuchi, K. *Polym. Degrad. Stab.* **1998**, *62*, 551.
28. Li, G.; Qi, R.; Lu, J.; Hu, X.; Luo, Y.; Jiang, P. *J. Appl. Polym. Sci.* **2013**, *127*, 3586.
29. Vanin, F. M.; Sobral, P. J. A.; Menegalli, F. C.; Carvalho, R. A.; Habitante, A. M. Q. B. *Food Hydrocoll.* **2005**, *19*, 899.

30. Bikiaris, D. N.; Papageorgiou, G. Z.; Achilias, D. S. *Polym. Degrad. Stab.* **2006**, *91*, 31.

31. Yasuniwa, M.; Tsubakihara, S.; Satou, T.; Iura, K. *J. Polym. Sci. Polym. Phys.* **2005**, *43*, 2039.

32. Yoo, E. S.; Im, S. S. *J. Polym. Sci. Polym. Phys.* **1999**, *37*, 1357.

33. Hassan, E.; Wei, Y.; Jiao, H.; Muhuo, Y. *J. Fiber Bioeng. Inform.* **2013**, *6*, 85.

34. Wu, D.; Yuan, L.; Lareda, E.; Zhang, M.; Zhou, W. *Indus. Eng. Chem. Res.* **2012**, *51*, 2290.

35. Iannace, S.; Ambrosio, L.; Huang, S. J.; Nicolais, L. J. *Appl. Polym. Sci.* **1994**, *54*, 1525.

36. Laun, H. M.; Munstedt, H. *Rheol. Acta* **1978**, *17*, 415.

37. Munstedt, H.; Laun, H. M. *Rheol. Acta* **1979**, *18*, 492.

38. Sato, Y.; Takikawa, T.; Sorakubo, A.; Takishima, S.; Masuoka, H.; Imaizumi, M. *Ind. Eng. Chem. Res.* **2000**, *39*, 4813.

39. Kazarian, S. G. *Polym. Sci. Ser. C* **2000**, *42*, 78.

40. Zullo, R.; Iannace, S. *Carbohydr. Polym.* **2009**, *77*, 376.